Biosensors and Bioelectronics 26 (2010) 36–42

Contents lists available at ScienceDirect

Biosensors and Bioelectronics

journal homepage: www.elsevier.com/locate/bios

Real-time monitoring and kinetic parameter estimation of the affinity interaction of jArtinM and rArtinM with peroxidase glycoprotein by the electrogravimetric technique

N.C. Pesquero[a], M.M. Pedroso[b], A.M. Watanabe[a], M.H.S. Goldman[c], R.C. Faria[b], M.C. Roque-Barreira[d], P.R. Bueno[a,*]

[a] Instituto de Química, Departamento de Físico-Química, Universidade Estadual Paulista, CP 355, 14800-900, Araraquara, São Paulo, Brazil
[b] Departamento de Química, Universidade Federal de São Carlos, CP 676, 13560-905, São Carlos, São Paulo, Brazil
[c] Departamento de Biologia, Faculdade de Filosofia Ciência e Letras de Ribeirão Preto, Universidade de São Paulo, Av. dos Bandeirantes, 3900, 14040-901, Ribeirão Preto, São Paulo, Brazil
[d] Departamento de Biologia Celular e Molecular e Bioagentes Patogênicos, Faculdade de Medicina de Ribeirão Preto, Universidade de São Paulo, Av. dos Bandeirantes, 3900, 14049-900, Ribeirão Preto, São Paulo, Brazil

ARTICLE INFO

Article history:
Received 5 March 2010
Received in revised form 28 April 2010
Accepted 30 April 2010
Available online 7 May 2010

Keywords:
Artocarpus integrifolia
ArtinM
Affinity equilibrium constant
Recombinant protein
Quartz Crystal Microbalance
Lectin

ABSTRACT

ArtinM is a D-mannose binding lectin that has been arousing increasing interest because of its biomedical properties, especially those involving the stimulation of Th1 immune response, which confers protection against intracellular pathogens. The potential pharmaceutical applications of ArtinM have motivated the production of its recombinant form (rArtinM) so that it is important to compare the sugar-binding properties of jArtinM and rArtinM in order to take better advantage of the potential applications of the recombinant lectin.

In this work, a biosensor framework based on a Quartz Crystal Microbalance was established with the purpose of making a comparative study of the activity of native and recombinant ArtinM protein. The QCM transducer was strategically functionalized to use a simple model of protein binding kinetics. This approach allowed for the determination of the binding/dissociation kinetics rate and affinity equilibrium constant of both forms of ArtinM with horseradish peroxidase glycoprotein (HRP), a N-glycosylated protein that contains the trimannoside Manα1–3[Manα1–6]Man, which is a known ligand for jArtinM (Jeyaprakash et al., 2004). Monitoring of the real-time binding of rArtinM shows that it was able to bind HRP, leading to an analytical curve similar to that of jArtinM, with statistically equivalent kinetic rates and affinity equilibrium constants for both forms of ArtinM. The lower reactivity of rArtinM with HRP than jArtinM was considered to be due to a difference in the number of Carbohydrate Recognition Domains (CRDs) per molecule of each lectin form rather than to a difference in the energy of binding per CRD of each lectin form.

1. Introduction

Lectins are non-catalytic proteins of non-immune origin that decode the information contained in complex carbohydrate structures of glycoproteins and glycolipids by stereo-specific recognition and binding. Lectin–carbohydrate interactions mediate several biological processes such as cell–cell recognition, host–pathogen interactions, cancer metastasis and cell differentiation. Although originally isolated and characterized from plants, lectins are found in different forms of life such as animals, plants, bacteria and viruses (Sharon, 2008).

Two lectins have been isolated from jackfruit seeds (*Artocarpus integrifolia*), jacalin and ArtinM (artocarpin or KM+) (Pereira-da-Silva et al., 2008). Jacalin, the first lectin to be isolated and characterized, binds D-galactose and has attracted considerable attention because of its ability to selectively recognize O-glycans associated to the hinge region of human IgA_1 (Kondoh et al., 1986; Roque-Barreira and Campos-Neto, 1985). ArtinM, in turn, binds to D-mannose and its administration to a mammalian host is followed by induction of Th1 immune response and protection against infection with intracellular pathogens. These properties are activated through the recognition of TLR2 glycans on phagocytes (Coltri et al., 2008) and the consequent induction of IL-12 production, a cytokine that favors the development of cell-mediated Th1 immunity (Panunto-Castelo et al., 2001), which is required to eliminate intracellular pathogens. In addition, ArtinM induces neutrophil migration through simultaneous interaction of its car-

* Corresponding author. Tel.: +55 16 3301 6643; fax: +55 16 3322 0015.
E-mail address: prbueno@iq.unesp.br (P.R. Bueno).

0956-5663/$ – see front matter © 2010 Elsevier B.V. All rights reserved.
doi:10.1016/j.bios.2010.04.047

bohydrate recognition domains (CRDs) with N-glycans linked to laminin (Ganiko et al., 2005) in the extracellular matrix and to receptor CXCR2 on the neutrophil surface (Pereira-Da-Silva et al., 2006), a property that contributes to the lectin's effect of conferring resistance to infections. Last but not least, the topical use of ArtinM accelerates tissue regeneration after burning (Pinto da Silva et al., 2004) and corneal wounds (Chahud et al., 2009).

ArtinM is a tetrameric non-glycosylated protein composed of identical 16 kDa protomers, each one consisting of a single polypeptide chain of 149 amino acid residues (Rosa et al., 1999). The protein CRDs (1 per protomer and 4 per whole protein) binds to D-mannose, preferentially recognizing N-linked glycans containing the trimannoside core Manα1–3[Manα1–6]Man (Jeyaprakash et al., 2004), such as those linked to the horseradish peroxidase (HRP), TLR2 (Coltri et al., 2008), laminin (Ganiko et al., 2005) and CXCR2 glycoproteins (Pereira-Da-Silva et al., 2006).

Current investigations into the properties of ArtinM (Chahud et al., 2009; Coltri et al., 2008; Ganiko et al., 1998, 2005; Panunto-Castelo et al., 2001; Pereira-Da-Silva et al., 2006; Rosa et al., 1999; Teixeira et al., 2006; Toledo et al., 2009) and, above all, its potential pharmaceutical applications, have been limited by the fact that this lectin corresponds to less than 0.5% of the total protein content of the extract of *A. integrifolia* seeds (Santos de Oliveira et al., 1994). Considering the interest in further exploring ArtinM properties, its cDNA was cloned and heterologously expressed in *S. cerevisae* and *Escherichia coli* (da Silva et al., 2005). The resulting recombinant forms of the protein (rArtinM) reproduced several biological properties of the native form (jArtinM) (Coltri et al., 2008). However, few studies to date have focused on the differences or equivalences of jArtinM and rArtinM.

Indeed, the analysis of sugar recognition by proteins has been gaining increasing importance in drug discovery. Efficient methods are required for fast and reliable recognition assays (Pei et al., 2005). Thus, electrogravimetric techniques, of which the Quartz Crystal Microbalance (QCM) technique is an example (Kanazawa and Gordon, 1985; Sauerbrey, 1959), have been used extensively in biorecognition analysis (Pedroso et al., 2008). The QCM technique also offers excellent advantages over traditional immune sensing techniques (ELISA and Surface Plasmon Resonance – SPR, etc.), providing rapid, cost-effective, highly sensitive and reliable results. Furthermore, QCM is able to measure tiny mass changes in real-time by label-free detection of molecules. The reliability of QCM measurements has been verified by other analytical methods such as impedance spectroscopy analysis, fluorescence spectroscopy, SPR, Atomic Force Microscopy (AFM) and photoelectron spectroscopy (Lebed et al., 2006).

The coupling of a biological sensing element to a transducer surface is the basis of biosensing (Gooding and Hibbert, 1999). Thus, QCM operates as a biological sensor that can be used in real-time studies of protein–carbohydrate binding and dissociation processes. The strategy consists in maintaining the biorecognition molecule close to the transducer surface while retaining its biological activity in a reproducible manner. Self-assembled monolayer (SAM) surfaces have been used in studies of molecular recognition for this purpose, since SAMs based on thiolates often constitute a base layer of controlled density which is well ordered, homogeneous, chemically and mechanically stable and which can be used to immobilize the biorecognition molecule. Particularly alkanethiols on gold electrodes of QCM transducers have been studied extensively, since the formation of the monolayer is achieved simply by immersing the substrate in an alkanethiol solution. In this context, proteins can be chemically bound via an adequate thiol head-group such as a carboxylic acid or an amine function (Mrksich and Whitesides, 1996; Ulman, 1996), leading to functionalized QCM transducers for a variety of studies and purposes. By means of a QCM transducer immobilization strategy, it is possible to monitor the binding kinetics, biomolecular affinity or kinetics of adsorption–desorption processes.

In the present work, the time courses of resonant frequency were identified during ArtinM–glycoprotein binding and as a result of the decreasing pattern of frequency over time, the mass increases of the sensor-induced surface resulting from the binding were inferred. Accordingly, the binding kinetics was derived. By fitting the experimental data to the kinetic model it was possible to estimate kinetic parameters such as binding and dissociation rate constants and the binding equilibrium constant of HRP (horseradish peroxidase) with both forms of ArtinM, i.e., native (jArtinM) and recombinant (rArtinM). The study provided relevant data concerning binding equivalences of jArtinM and rArtinM.

2. Experimental

2.1. Reagents and solutions

The lectin jArtinM (native lectin) used in this work was extracted from *A. integrifolia* seeds and isolated by affinity chromatography to immobilized D-mannose, as previously described (Santos de Oliveira et al., 1994). In the case of rArtinM, it has been isolated through the same affinity procedure from cultures of *E. coli* BL21 (DE3) Codon Plus-RP transformed with pEXP-KM$^+$ (da Silva et al., 2005), i.e. from clones encoding the full-length ArtinM primary sequence from a cDNA library, through matrix PCR-based screening methodology. The bacterial cells were sonicated and spun at 25,000 × *g* for 15 min. The soluble proteins were affinity-purified on a D-mannose column from the supernatant produced after sonication.

Confirming previous results (Coltri et al., 2008; da Silva et al., 2005; Santos de Oliveira et al., 1994), the procedure led to a system that was able not only to produce a good protein yield of 16 kDa pure protein but also a functional lectin, since rArtinM was able to bind dose-dependently to horseradish peroxidase (HRP), as observed through a microplate binding assay. Therefore, in the present work, HRP supplied by Sigma Chemical Co. (St. Louis, MO, USA) was used to evaluate native and recombinant ArtinM binding properties. Gelatin, also from Sigma Chemical Co. (St. Louis, MO, USA), was used after the protein immobilization to react with the residual terminal carboxylic group of 11-mercaptoundecanoic acid as a blocking reagent of the functionalized QCM piezoelectric transducer surface (see supplementary materials).

All the solutions used in the analytical procedures were prepared with Milli-Q purified water (Millipore system, Bedford, MA, USA) with 18 MΩ. The ArtinM solutions (native and recombinant) were prepared and used in 0.10 M phosphate buffered solution, pH 7.4, with 0.15 M of NaCl (PBS).

2.2. Apparatus

The quartz used was 16 mm in diameter, AT-cut, and had a fundamental frequency of 5 MHz (polished quartz crystals provided by Q-SENSE company with gold electrodes). Prior to the experiments, the quartz electrode surface was cleaned with a solution of freshly prepared 7:3 H_2SO_4 (conc.):H_2O_2 30% (v/v), rinsed with water and dried in air. The crystal was then placed in a Q-SENSE cell with one face in contact with the solution and the other exposed to air. The measurements were performed in a Q-SENSE E4 Quartz Crystal Microbalance (QCM system), using an ISMATEC IPC peristaltic pump with a controlled constant flow of 200 μL min^{-1}.

2.3. Lectin immobilization methodology

The methodology employed for lectin immobilization was based on multilayer assembly on the gold surface of a piezo-

electric transducer quartz crystal. The cleaned piezoelectric quartz crystal was incubated for 3 h in a solution containing 1.0×10^{-4} mol L^{-1} 11-mercaptoundecanoic acid (MUA) and 10 mol L^{-1} of 2-mercaptoethanol in ethanol as solvent. The crystal was then washed with ethanol and PBS. After this, the quartz crystal was incubated for 2 h in EDC/NHS solution 1.0×10^{-2} and 2.0×10^{-2} mol L^{-1}, respectively, after which it was washed with PBS. Finally, the quartz crystal was exposed to the lectin solutions (0.15 mg mL^{-1} of ArtinM) for 2 h and then rinsed with PBS. To block residual carboxylic groups, the lectin-modified crystal surface was exposed to a gelatin solution at 0.001% (w/v) for 1 min and washed with PBS.

2.4. Electrochemistry measurements

The electrochemical experiments were carried out in a typical three electrode cell at ambient temperature, where the working electrode was the gold functionalized surface. A platinum plate was the counter electrode and saturated calomel electrode was used as the reference. The cyclic voltammetric experiments were carried out by means of a potentiostat-galvanostat (AUTOLAB PGSTAT30). The working electrode was immersed into 25 μmol L^{-1} hydroquinone environment (Sigma Chemical Co.) and 850 μmol L^{-1} of H_2O_2 (Synth).

3. Results and discussion

3.1. Validation of the jArtinM and rArtinM binding specificity

The ArtinM functionalized quartz crystal was placed in the Q-SENSE cell under a continuous PBS flux until the frequency signal stabilized. The minimum (precision signal detection of the system) and maximum (saturation of the surface) detectable signal of HRP with the ArtinM functionalized quartz crystal were examined by sweeping the HRP concentration. The real-time binding study involved adding different concentrations of HRP to the two functionalized electrodes containing jArtinM and rArtinM. The real-time frequency response curves of two distinct HRP concentrations are shown in Fig. 1. The HRP injection into the cell (indicated by arrows) caused the crystal frequency to decrease, indicating HRP binding to ArtinM immobilized on the transducer surface. When the PBS fluxes started (indicated by arrows) the resonant frequency increased, and the difference between the stable original and final values corresponded to the frequency shift due to covalent binding of HRP and ArtinM with the contribution of a non-specific interaction.

It is important to emphasize that the final variation of the quartz crystal frequency was the same for native and recombinant lectins. These results indicate that the active sites are the same for both forms of the lectin. Accordingly, the real-time binding did not show differences between HRP binding to the immobilized surface of jArtinM and of rArtinM. Apparently, the binding pattern up to stabilization depends on the concentration of HRP on the medium.

The ArtinM binding specificity to HRP was confirmed for both native and recombinant lectins, using BSA as negative control. BSA was immobilized in the quartz transducer in place of lectin and HRP was added in the maximum saturation concentration previously established, i.e., 1.0 mmol L^{-1} (not shown). This measurement was taken in triplicate and the frequency variation of the quartz crystal was about 3 ± 2 Hz. This result demonstrates that BSA, a non-glycosylated protein, does not interact with ArtinM, as expected.

Cyclic voltammetry (CV) was performed to obtain additional information about binding and interaction of HRP with jArtinM and rArtinM. The measurements were based on the fact that HRP is able to reduce H_2O_2 mechanistically, as illustrated in supplementary material. The CV measurements for different functionalized transducers were examined: (a) jArtinM and (b) rArtinM functionalized electrodes. CV measurements were also taken of HRP modified electrodes in pure PBS solution (as blank test) and PBS solution in the presence of hydroquinone and hydrogen peroxide. All the proteins were immobilized on the quartz crystal by means of MUA, as described in Section 2.3. The CV measurements on the functionalized transducer were taken before and after the HRP reactions (see Fig. 2).

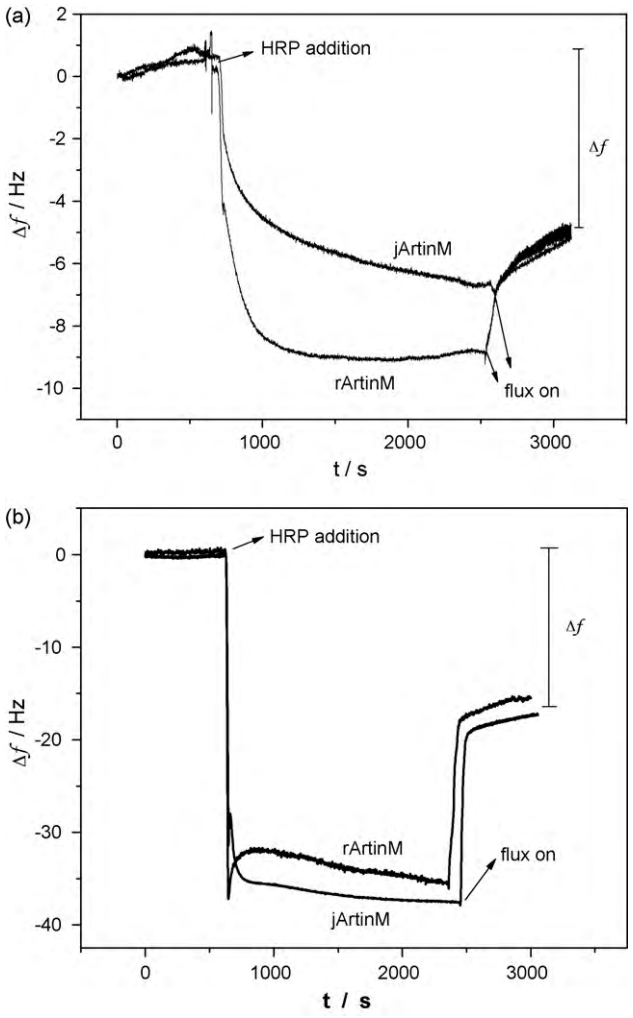

Fig. 1. Real-time frequency (Δf) shifts as a function of measured time of ArtinM–HRP binding at different concentrations of HPR bulk or solution: (a) 0.15 mmol L^{-1} and (b) 1.5 mmol L^{-1}.

Fig. 2d shows the CV measurements obtained with HRP immobilized in two different electrolyte environments. Note the cathodic current when HRP is present due to a small charge transfer of H_2O_2 reaction with HRP enzyme (Damos et al., 2004). The transducers functionalized with jArtinM and rArtinM were immersed in HRP 1.0 mmol L^{-1} solution for 30 min. The transducer electrode was washed with PBS solution prior to taking the CV measurements. The CV measurements of transducers containing immobilized jArtinM and rArtinM are depicted in Fig. 2a and b. Fig. 2c compares CV measurements of jArtinM and rArtinM modified electrodes. Based on the results, it can be stated that both native and recombinant lectins are active and interact with HRP. This is confirmed by the increasing cathodic current values (Fig. 2), which indicate that H_2O_2 is more strongly reduced in the presence of lectin–HRP complexes than solely in that of HRP.

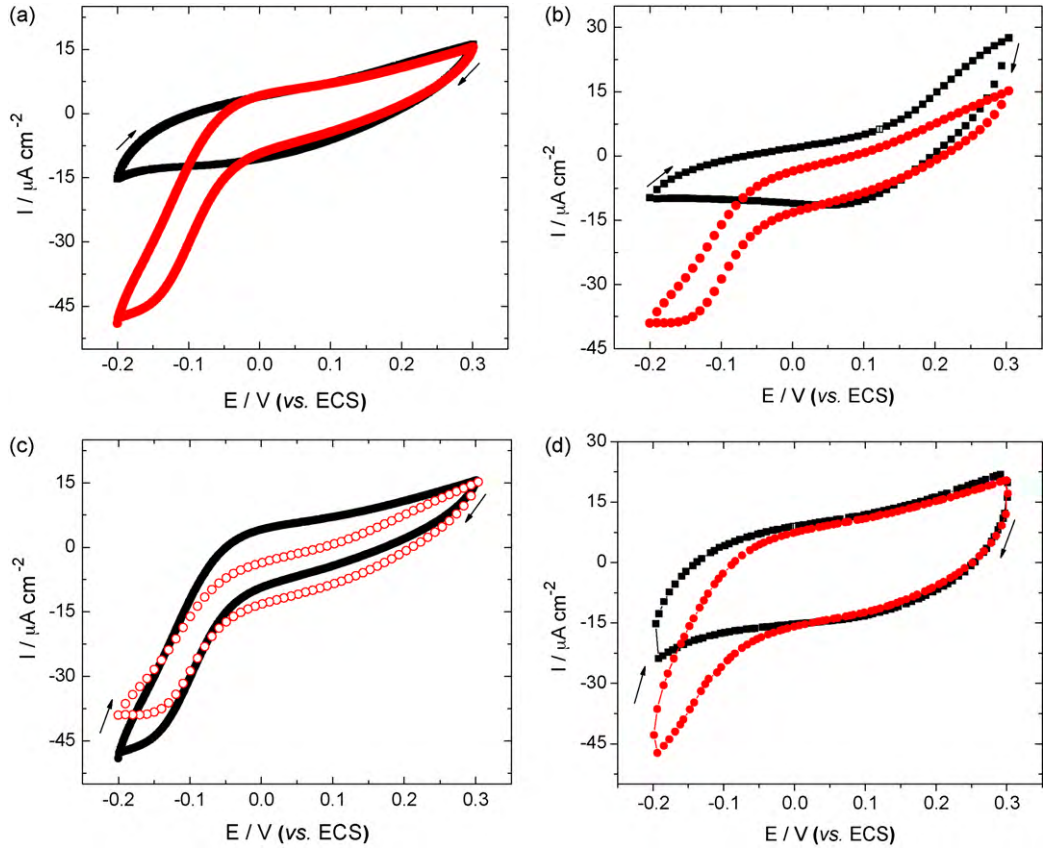

Fig. 2. (a) Cyclic voltammetry of gold modified electrode with jArtinM after 30 min of interaction with HPR in 0.5 mmol L^{-1}: (■) in 0.1 mol L^{-1} PBS solution and (●) in hydroquinone 0.25 μmol L^{-1} and H_2O_2 850 μmol L^{-1} in PBS solution. (b) Cyclic voltammetry of gold modified electrode with rArtinM after 30 min of interaction with HPR in 0.5 mmol L^{-1}: (■) in 0.1 mol L^{-1} PBS solution and (●) in hydroquinone 0.25 μmol L^{-1} and H_2O_2 850 μmol L^{-1} in PBS solution. (c) Comparison of (■) jArtinM e (○) rArtinM. (d) Cyclic voltammetry of Au modified electrode with HRP 1.0 mmol L^{-1} in (■) 0.1 mol L^{-1} PBS solution and (●) in hydroquinone 0.25 μmol L^{-1} and H_2O_2 850 μmol L^{-1} in PBS solution.

Therefore, it is important to emphasize that the cathodic current of jArtinM is equivalent to the current obtained for rArtinM. This result is particularly interesting in light of our recent finding that rArtinM, expressed by transformed *E. coli*, seems to be monomeric, in contrast to the tetrameric structure of jArtinM (Rosa et al., 1999).

3.2. Kinetic model and parameter estimation for the binding/dissociation process

The kinetics of the adsorption process is related to the change in free energy of protein adsorption. The kinetics may also provide information about the sequence in which different sub-processes occur during adsorption. In the simplest protein adsorption model, the adsorption species are assumed to be rigid, to bind reversibly with homogeneous binding energies, and not to interact with each other. In such a situation, it is possible to calculate theoretically the binding affinity, K (which is the ratio between the rate constant for adsorption or binding and the desorption or dissociation) directly from the amount of binding, Γ, at a given protein bulk concentration [ ], or from a mathematical fit to a kinetic curve pattern, i.e., Γ *versus* time.

To ensure the above condition for the kinetic model, it is possible to design the biosensor or QCM functionalized surface strategically to satisfy the model's boundary condition. Therefore, to ensure that a critical point related to the rigidity of the protein layer and the interactivity of each unit would be reached, a homogeneous self-assembled monolayer was constructed, as described in Section 2, consisting of two alkanethiols, i.e., MUA and 2-mercaptoethanol in a proportion of 1:100,000, respectively. The MUA was used for lectin binding and immobilization on the transducer surface by means of the amine group present in the lectin structure with the carboxyl group present in the MUA. Thus, the 2-mercaptoethanol served as a spacing layer, i.e., to space the immobilized lectin molecules. Due to the amount of 1:100,000, it can be seen that the transducer's functional surface provided a sufficient distance (very thin surface coating) between similar units of HRP binding on the transducer surface to prevent cross interaction between HRP molecules, thus increasing the possibility of rigidity and homogeneous binding energy. Furthermore, it is known that the lectin–glycoprotein interaction is reversible and kinetically rapid, allowing mass transport to be neglected.

Details on the kinetic binding and dissociation using our nomenclature for the reaction of HRP with immobilized ArtinM on the piezoelectric transducer is shown in detail in Appendix A, and the transducer's response is associated with the kinetic binding according to the model presented there.

3.3. Binding and dissociation rate constants and binding equilibrium constant

Eq. (A.11) was used to calculate and estimate both binding and dissociation rates of the interaction between ArtinM lectins and HRP glycoprotein. In the first step, the oscillation frequency of the quartz crystal as a function of different glycoprotein concentration was recorded. The real-time relaxation curves were recorded for jArtinM and rArtinM. The measurements and curves were made in triplicate and are shown in Fig. 3, illustrating the real-time relaxation curves of HRP interaction with jArtinM and rArtinM

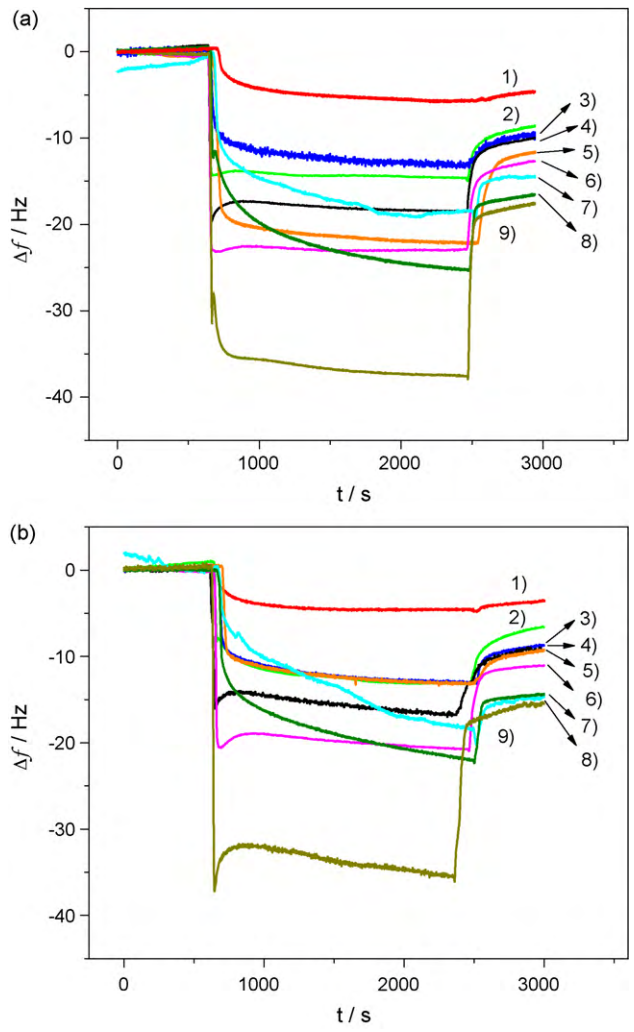

Fig. 3. Real-time relaxation curves (Δf shifts as a function of time) for different HPR concentrations: (a) jArtinM, and (b) rArtinM. (1)–(7) indicate the respective curves (in increasing order of concentration) for the HRP concentrations indicated in Table 1. (8) and (9) depict the saturated HRP concentrations of 1.0 and 1.5 mmol L^{-1}, respectively. These are mean value curves since they were obtained in triplicate.

immobilized on the quartz crystal transducer surface at different concentrations of HRP glycoprotein (only the mean values, i.e., the mean curves are shown). The relaxation curves in Fig. 3 were adjusted statistically to Eq. (A.11) and the τ^{-1} values for each HRP concentration and the binding processes at different HRP concentrations were monitored in the same physicochemical conditions, resulting in a series of τ^{-1} (example of the fitting are given in supplementary material). Table 1 lists the values of relaxation time constant obtained for jArtinM and rArtinM.

Table 1
Mean values of reciprocal or characteristic relaxation time (τ^{-1}) of ArtinM–HRP binding reaction to native and recombinant lectins. The mean values of τ^{-1} (characteristic frequency) are shown for different bulk or solution concentrations.

[HRP]/mmol L^{-1}	jArtinM $\tau^{-1}{}_{mean}$ ($\times 10^{-3}$)/s^{-1}	rArtinM $\tau^{-1}{}_{mean}$ ($\times 10^{-3}$)/s^{-1}
0.15	6 ± 1	8 ± 1
0.22	12 ± 1	9 ± 1
0.30	13 ± 1	13 ± 1
0.40	17 ± 1	15 ± 1
0.50	15 ± 1	17 ± 1
0.65	24 ± 1	22 ± 2
0.75	24 ± 1	23 ± 2

Table 2
Kinetic constant rates of binding and dissociation and kinetic equilibrium affinity constant for jArtinM–HRP and rArtinM–HRP.

Interaction	k_1/L mol^{-1} s^{-1}	k_{-1}/s^{-1}	K_a/L mol^{-1}
jArtinM–HRP	28 ± 4	$(4 \pm 2) \times 10^{-3}$	$(7 \pm 3) \times 10^3$
rArtinM–HRP	27 ± 2	$(4 \pm 1) \times 10^{-3}$	$(7 \pm 2) \times 10^3$

The second step consisted of plotting the relaxation time constant of the reaction as a function of HRP concentration, whose curves are shown in Fig. 4. Therefore, Eq. (A.13), which indicates the relationship between the relaxation rate constant and the initial HRP concentration, was used to calculate the k_1 and k_{-1} kinetic parameters using the angular and linear coefficients of the linear plots, respectively.

Finally, based on the k_1 and k_{-1} kinetic parameters, the binding equilibrium constant, K_a, was calculated as:

$$K_a = \frac{k_1}{k_{-1}} \tag{1}$$

Therefore, the binding equilibrium constants for jArtinM and rArtinM were calculated from Eq. (1), and are shown in Table 2. Note that jArtinM–HRP and rArtinM–HRP have the same binding equilibrium constants, despite the structural differences between native and recombinant ArtinM lectins. Therefore, it is possible to infer that the binding sites of jArtinM and rArtinM are the same and the structural differences correspond to the number of sites.

3.4. Binding and dissociation rate constants and apparent affinity constant

Considering the kinetic model of Eq. (A.1) and the validity of the boundary conditions established previously, the apparent affinity constant can also be calculated alternatively, according to Eqs. (A.2) and (A.3) and Eqs. (A.9)–(A.11), by means of:

$$\frac{\Gamma_b}{\Gamma_{b,e}} = \frac{\Delta f_0}{\Delta f_{max}} = \frac{K_a[HRP]}{1 + K_a[HRP]} \tag{2}$$

which is equivalent, but sometimes referred to as the apparent affinity constant, since the methodology depends directly on the equilibrium concentration of the binding process. Therefore, if it is plotted according to Eq. (2), the [HRP]/Δf_0 as a function of [HRP], the K_a values can be calculated directly from the slope of these curves. The curves found in this work are shown in Fig. 4c and d the values found here were $(4.6 \pm 0.9) \times 10^3$ and $(2.6 \pm 0.5) \times 10^3$ L mol^{-1}, respectively, for jArtinM–HRP and rArtinM–HRP.

4. Final remarks and conclusions

The electrogravimetric analysis performed in this work, allied to a simple kinetic model for HRP binding with two forms of ArtinM lectins, i.e., native and recombinant, enabled us to establish an equivalence for the kinetics of binding/association affinity of the ligand sites of these proteins. These results are relevant because they demonstrate that the specificity of glycan recognition of rArtinM is equivalent to the specificity of jArtinM.

The remarkable similarity in the data obtained by the electrogravimetric and electrochemical approaches indicates this equivalence. In electrochemical analysis, the equivalence was evidenced by the ability of HRP to reduce H_2O_2 at 1 mmol L^{-1}, confirming that HRP binds equally to both ArtinM structures. Evidently, these are the same conditions established for electrogravimetric analysis, where the system reaches the condition of equilibrium according to its relaxation time constant, i.e., τ.

Therefore, the equivalence of the τ value for rArtinM and jArtinM indicates that the diluted coating of the transducer surface with

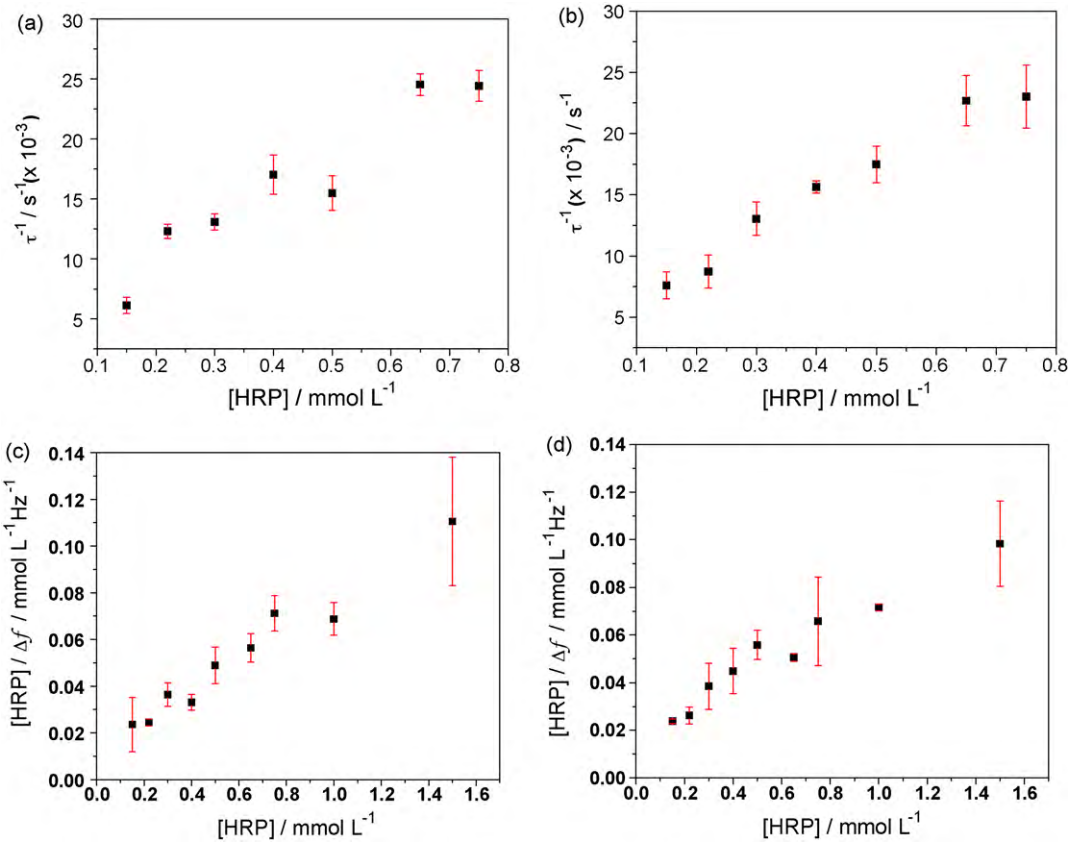

Fig. 4. Linear relationship between τ^{-1} *versus* [HRP] and linear relationship between the [HRP]/Δf ratio and [HRP]. The pattern of these curves follows Eqs. (A.13) and (A.15), respectively. It was possible to calculate the binding and dissociation kinetic constant rates for (a) jArtinM, and (b) rArtinM; and to calculate the equilibrium concentration of the binding process for (c) jArtinM, and (d) rArtinM.

rArtinM and jArtinM leads to a binding regime in which the boundary conditions of the classical protein binding model are effectively satisfied (which cannot be a general conclusion, since the behavior of both rArtinM and jArtinM under non-diluted conditions could be different). Finally, the K_a, i.e., the apparent affinity constant, was calculated by two different methodologies, i.e., by means of the τ value, which is influenced by the non-specific bonds, and the classical method represented in Eq. (15), which takes into account only the high specific bonds of the interaction. In both cases, the K_a values were found to be equivalent for jArtinM and rArtinM, and the two methodologies yielded very similar values.

It is important to discuss about the differences on the methodologies used for calculation of kinetic constants and K_a values. The second method yielded much lower K_a values differing by almost a factor of two for jArtinM and rArtinM. From the procedures and results discussed previously it is possible to note that in the first methodology, there is no influence of non-specific binding while in the second it is present. Therefore, the observed differences between values obtained from one method to the other can be attributed to the influence of non-specific binding. Therefore, the comparison between the values obtained of a particular methodology permit to infer that non-specific binding influences equally the kinetic values over the specific binding of two jArtinM and rArtinM lectins with HRP so that the kinetic values between both protein does not vary comparatively (for the same method used).

A detailed understanding of the sugar-binding features of ArtinM provides a solid basis for its application as an agent of tissue regeneration after burning and immunomodulation against intracellular pathogens. The comparison of the jArtinM and rArtinM results allows for validation of the use of the recombinant form in place of the native form as a therapeutic tool that can compensate for the limited availability of plant-derived lectin and the low yields obtained from lectin purification.

Acknowledgements

The authors acknowledge the support of this work by the São Paulo State Research Funding Agency (FAPESP) and the National Research Council (CNPq). We are indebted to Sandra Maria de Oliveira Thomaz for her careful purification of the ArtinMs used in this work.

Appendix A.

The simplest kinetic mode can be given by Mao et al. (2002) and Nilsson (2007):

$$[\text{free ArtinM site}]_s + [\text{HRP}]_l \underset{k_{-1}}{\overset{k_1}{\rightleftarrows}} [\text{HRP-bound site}]_s \quad (A.1)$$

in which $[\,]_s$ and $[\,]_l$ indicate the concentration on the surface of the piezoelectric sensor and in solution, respectively. k_1 and k_{-1} are, respectively, the binding and dissociation rate constants (HRP binding sites in ArtinM). The binding and dissociation rates (r_b and r_d) of the binding species can be defined as:

$$r_b = k_1 \Gamma_f [\text{HRP}], \quad (A.2)$$

$$r_d = k_{-1} \Gamma_b. \quad (A.3)$$

Assuming that the total number of sites for binding is given by N, the percentage of free sites for binding, i.e., free n_f sites, is given by $\Gamma_f = n_f/N$, in which n_f is the number of free sites and Γ_f is the free

site fraction (non-binding) or percentage. Similarly, the occupation or percentage of binding sites will be given by $\Gamma_b = n_b/N$, where n_b is the number of binding sites. In other words, Γ_f and Γ_b indicate the percentage, respectively, of the remaining free-binding sites that can bind with HRP and of the HRP–ArtinM sites on the surface at time t.

When the system reaches equilibrium, $r_b = r_d = r_e$, which is (Mao et al., 2002),

$$r_e = k_1 \Gamma_{f,e} [\mathrm{HRP}]_e = k_{-1} \Gamma_{b,e} \tag{A.4}$$

where the subscript e represents the amount at equilibrium time. If δ is the relaxation variable of the equilibrium system, then

$$\delta = \Gamma_f - \Gamma_{f,e} = [\mathrm{HRP}] - [\mathrm{HRP}]_e = \Gamma_{b,e} - \Gamma_b \tag{A.5}$$

The reaction rate of deviation from the equilibrium $d\delta/dt$ is

$$-\frac{d\delta}{dt} = k_1(\Gamma_{f,e} + \delta)([\mathrm{HRP}]_e + \delta) - k_{-1}(\Gamma_{b,e} - \delta) \tag{A.6}$$

The term δ^2 can be disregarded because δ is often a small value. Hence, Eq. (A.6) can be simplified as

$$-\frac{d\delta}{dt} = \left(\frac{1}{\tau}\right)\delta \tag{A.7}$$

where

$$\frac{1}{\tau} = r_e \left(\frac{1}{\Gamma_{f,e}} + \frac{1}{[\mathrm{HRP}]_e} + \frac{1}{\Gamma_{b,e}}\right) \tag{A.8}$$

which is the relaxation rate constant, while τ is known as the relaxation time. The combined solution of Eqs. (A.7) and (A.5) gives

$$\Gamma_b = \Gamma_{b,e}\left(1 - e^{-(1/\tau)t}\right) \tag{A.9}$$

The equilibrium percentage $\Gamma_{b,e}$ corresponds to the maximum percentage of active HRP-bound sites. Moreover, an increase in $\Gamma_{b,e}$ must result in a mass increase of the sensor surface. The value of $\Gamma_{b,e}$ is proportional to the mass increase, Δm. Therefore, the following can be expected:

$$\Delta m_t = \Delta m_{\max}\left(1 - e^{-(1/\tau)t}\right) \tag{A.10}$$

where Δm_t and $\Delta m_{\max}$ are the mass increase of the sensor surface at time t and $t \to \infty$ (or at the time of binding equilibrium), respectively. The decrease in frequency should be ascribed mainly to the mass increase resulting from binding. Although the Sauerbrey equation cannot strictly be used to describe the relationship between Δf_0 and Δm when the sensor is in liquid, there is a positive relevance between these two parameters. Furthermore, if the values of Δf_0 resulting from the binding are not too high (e.g., lower than 40 Hz in this work), it is reasonable to assume that Δm is proportional to Δf_0 in such a small range. Thus, Eq. (A.10) can be rewritten as

$$\Delta f_0 = \Delta f_{\max}\left(1 - e^{-(1/\tau)t}\right) \tag{A.11}$$

where Δf_0 and $\Delta f_{\max}$ are the frequency changes at time t and $t \to \infty$, respectively. This equation can be considered the piezoelectric response model during binding, and can be used to describe the kinetics of the binding process.

From Eqs. (A.4) and (A.8) we can derive the following equation:

$$\tau^{-1} = k_1([\mathrm{HRP}]_e + \Gamma_{f,e}) + k_{-1} \tag{A.12}$$

It can be assumed that the initial concentration of HRP ($[\mathrm{HRP}]_0$) is much larger than the concentration of HRP consumed by binding, or $[\mathrm{HRP}]_e \approx [\mathrm{HRP}]_0$. In addition, $\Gamma_{f,e} \to 0$ when $t \to \infty$ because the free-binding sites in ArtinM on the sensor surface will change to HRP-bound sites as binding proceeds. Therefore, Eq. (A.12) can be simplified to

$$\tau^{-1} = k_1[\mathrm{HRP}] + k_{-1} \tag{A.13}$$

Appendix B. Supplementary data

Supplementary data associated with this article can be found, in the online version, at doi:10.1016/j.bios.2010.04.047.

References

Chahud, F., Ramalho, L.N.Z., Ramalho, F.S., Haddad, A., Roque-Barreira, M.C., 2009. International Journal of Experimental Pathology 90 (2), 166–173.

Coltri, K.C., Oliveira, L.L., Pinzan, C.F., Vendruscolo, P.E., Martinez, R., Goldman, M.H., Panunto-Castelo, A., Roque-Barreira, M.C., 2008. American Journal of Pathology 173 (2), 423–432.

da Silva, L.L., Molfetta-Machado, J.B., Panunto-Castelo, A., Denecke, J., Goldman, G.H., Roque-Barreira, M.C., Goldman, M.H., 2005. Biochimica et Biophysica Acta 1726 (3), 251–260.

Damos, F.S., Mendes, R.K., Kubota, L.T., 2004. Quimica Nova 27 (6), 970–979.

Ganiko, L., Martins, A.R., Espreafico, E.M., Roque-Barreira, M.C., 1998. Glycoconjugate Journal 15 (5), 527–530.

Ganiko, L., Martins, A.R., Freymuller, E., Mortara, R.A., Roque-Barreira, M.C., 2005. Biochimica et Biophysica Acta-General Subjects 1721, 152–163.

Gooding, J.J., Hibbert, D.B., 1999. Trends in Analytical Chemistry 18 (8).

Jeyaprakash, A.A., Srivastav, A., Surolia, A., Vijayan, M., 2004. Journal of Molecular Biology 338, 757–770.

Kanazawa, K.K., Gordon, J.G., 1985. Analytical Chemistry 57, 1770.

Kondoh, H., Kobayashi, K., Hagiwara, K., Kajii, T., 1986. Journal of Immunological Methods 88, 171.

Lebed, K., Kulik, A.J., Forró, L., Lekka, M., 2006. Journal of Colloid and Interface Science 299, 41–48.

Mao, Y.A., Wei, W.Z., He, D.L., Nie, L.H., Yao, S.Z., 2002. Analytical Biochemistry 306 (1), 23–30.

Mrksich, M., Whitesides, G.M., 1996. Annual Review of Biophysics and Biomolecular Structure 25, 55–78.

Nilsson, C.L., 2007. Lectins: Analytical Technologies, 2nd ed. Elsevier, Amsterdam.

Panunto-Castelo, A., Souza, M.A., Roque-Barreira, M.C., Silva, J.S., 2001. Glycobiology 11 (12), 1035–1042.

Pedroso, M.M., Watanabe, A.M., Roque-Barreira, M.C., Bueno, P.R., Faria, R.C., 2008. Microchemical Journal 89 (2), 153–158.

Pei, Z.C., Anderson, H., Aastrup, T., Ramstrom, O., 2005. Biosensors & Bioelectronics 21 (1), 60–66.

Pereira-Da-Silva, G., Moreno, A.N., Marques, F., Oliver, C., Jamur, M.C., Panunto-Castelo, A., Roque-Barreira, M.C., 2006. Biochimica et Biophysica Acta-General Subjects 1760 (1), 86–94.

Pereira-da-Silva, G., Roque-Barreira, M.C., Van Damme, E.J.M., 2008. Immunology Letters 119, 114–115.

Pinto da Silva, L.L., Panunto-Castelo, A., de Souza Goldman, M.H., Roque Antunes Barreira, M., de Oliveira, R.S., Dias Baruffi, M., Blanco de Molfetta Machado, J., Santos de Oliveira, R., 2004. Patent International Application No. PCT/BR2004/000870.

Roque-Barreira, M.C., Campos-Neto, A., 1985. The Journal of Immunology 134 (3), 1740–1743.

Rosa, J.C., de Oliveira, P.S.L., Garratt, R., Beltramini, L., Resing, K., Roque-Barreira, M.C., Greene, L.J., 1999. Protein Science 8 (1), 13–24.

Santos de Oliveira, R., Dias Baruffi, M., Thomaz, S.M.O., Beltramini, L.M., Roque-Barreira, M.C., 1994. Journal of Immunology 153 (4), 1798–1807.

Sauerbrey, G., 1959. Zeitschrift Fur Physik 155, 206–222.

Sharon, N., 2008. Biochemical Society Transactions 36, 1457–1460.

Teixeira, C.R., Cavassani, K.A., Gomes, R.B., Teixeira, M.J., Roque-Barreira, M.C., Cavada, B.S., da Silva, J.S., Barral, A., Barral-Netto, M., 2006. Vaccine 24 (15), 3001–3008.

Toledo, K.A., Scwartz, C., Oliveira, A.F., Conrado, M., Bernardes, E.S., Fernandes, L.C., Roque-Barreira, M.C., Pereira-da-Silva, G., Moreno, A.N., 2009. Immunology Letters 123 (1), 14–20.

Ulman, A., 1996. Chemical Reviews 96 (4), 1533–1554.